J. Fluid Mech. (1982), *vol.* 121, *pp.* 123–140
Printed in Great Britain

Reynolds-number dependence of the structure of a turbulent boundary layer

By R. A. ANTONIA, S. RAJAGOPALAN, C. S. SUBRAMANIAN AND A. J. CHAMBERS

Department of Mechanical Engineering, University of Newcastle, N.S.W., 2308, Australia

(Received 31 July 1981 and in revised form 4 January 1982)

Conditional averages of longitudinal, normal velocity and temperature fluctuations and of their products have been obtained in a slightly heated boundary layer with zero pressure gradient over a momentum-thickness Reynolds-number range $990 \leqslant R_{\mathrm{m}} \leqslant 7100$. These averages are based on the identification of coherent temperature fronts that extend across most of the layer. The average period between fronts is approximately independent of R_{m} when R_{m} is greater than about 1500. The streamwise length scale of the fronts and the magnitude of velocity and temperature derivatives associated with the fronts scale on the thickness of the layer except for R_{m} less than about 3000. This scaling is consistent with the Reynolds-number independence, for R_{m} greater than about 3000, of both mean and turbulent velocity and temperature fields. Conditional averages are discussed in the context of Head & Bandyopadhyay's (1978) suggestion, based on smoke-flow visualization, that the boundary layer consists almost exclusively of hairpin eddies.

1. Introduction

The influence of Reynolds number on the mean-velocity field of a turbulent boundary layer is sufficiently documented in the literature. Coles (1962) noted that the 'wake' component in the outer part of the boundary layer is approximately independent of the Reynolds number when R_{m} exceeds about 5000.† The possibility that the low-Reynolds-number effects may be due to the Reynolds-number dependence of the log-law constants rather than a breakdown of outer-layer similarity has been dismissed by Huffman & Bradshaw (1972), and is not supported by the measurements of Murlis (1975), Purtell (1978), Purtell, Klebanoff & Buckley (1981) and Subramanian & Antonia (1981). These measurements, at least to within the experimental uncertainty, confirm that the log-law constants are universal for values of R_{m} as small as 500. Huffman & Bradshaw (1972) have suggested that the R_{m} dependence of the 'wake' component may be attributed to the increased importance of the viscous superlayer with decreasing R_{m}. Photographs and films of a smoke-filled boundary layer (Falco 1974; Head & Bandyopadhyay 1978, 1979, 1981) show that the turbulent/non-turbulent interface of the layer becomes more convoluted and extends down to the wall as R_{m} decreases, and therefore seem to reinforce the suggestion that viscous effects in the outer layer may reflect the influence of the superlayer.

† Although R_θ is the more usual symbol for the momentum-thickness Reynolds number, the subscript m is used here since θ denotes the temperature fluctuation.

Purtell's (1978) outer-layer distributions of the r.m.s. longitudinal velocity show a fair degree of similarity in the range $465 < R_m < 5100$ when scaled with outer-layer variables. In the outer layer ($y/\delta \gtrsim 0{\cdot}2$, where δ is the boundary-layer thickness) δ may be regarded as a characteristic length scale, while either the free-stream velocity U_1 or friction velocity U_τ may be considered as an appropriate characteristic velocity. There is mixed evidence for the effect of R_m on turbulence structure parameters. Murlis, Tsai & Bradshaw (1980) noted that the ratio $\overline{u^2}/\overline{v^2}$ (u and v are velocity fluctuations in the x- and y-directions) changes quite rapidly for $R_m < 2000$, but third-order moments, derived from u and v, are not significantly affected by R_m when normalized by the Reynolds shear stress.

The effect of R_m on the turbulence structure, as inferred from the smoke-flow visualization of Falco (1974) and Head & Bandyopadhyay (1978, 1981) is more spectacular than that inferred from the previously mentioned hot-wire measurements. Falco (1974) recognized a family of events, described as typical eddies, over a relatively large range of R_m. At $R_m = 600$, the length scale of these eddies was of order δ and the eddies were identified with the large eddies. At $R_m \simeq 6000$ Falco found that the typical eddy scales were an order of magnitude smaller than δ and noted the appearance of concentration gradients extending across most of the layer. He also suggested that entrainment of non-turbulent fluid would occur on typical eddy rather than on outer-layer length scales. By combining hot-wire measurements with flow visualization, Falco (1977) obtained signatures of u, v and the product uv associated with the typical eddy. From the uv-signature at $R_m \simeq 1200$ he inferred that typical eddies made a significant contribution to the Reynolds shear stress. Since the typical eddy scaled on wall variables in the range $900 \lesssim R_m \lesssim 20000$, Falco's results seem to imply that part of the motion that contributes significantly to the shear stress depends significantly on Reynolds number. This implication would appear to be in conflict with the previous measurements of the mean velocity and turbulent quantities, at least when R_m is greater than about 5000. The flow-visualization experiments of Head & Bandyopadhyay (1978, 1979, 1981) indicate, perhaps not surprisingly, that there is little distinction for $R_m \lesssim 500$ between large- and small-scale motions, the large eddies consisting of hairpin† vortices appearing either individually or in relatively small groups. At higher R_m the large structure is made up of random agglomerations of hairpin vortices. Occasionally, a regular sequence of hairpin vortices is formed (see also Bandyopadhyay 1980) so that their tips, perhaps identifiable with the typical eddies, lie on a line which makes a smaller angle to the surface than the 45° angle characteristic of the hairpin eddies.

In the present paper, the influence of Reynolds number on the turbulence structure is examined by considering the effect of R_m on conditional averages of u, v, the temperature fluctuation θ, and of their products. These averages are associated with the temperature fronts (Chen & Blackwelder 1978 – their terminology is retained here) which extend across the entire logarithmic region of the layer and are always identified with the backs of bulges in the intermittent region of the layer. The conditional technique is briefly described in §3. Results obtained with the technique are presented in §§4 and 5 and discussed in the context of the information already obtained for

† These authors distinguished between vortex loops at very low R_m, horseshoes at low–moderate R_m and elongated hairpin eddies or vortex pairs at high R_m. This distinction is not made in the present paper.

U_1 (m s^{-1})	R_m	δ (cm)	δ_T (cm)	δ_s (cm)	U_τ (m s^{-1})	T_τ (°C)	c_f present	c_f Coles (1962)	f_s (kHz)
2·1	990	5·4	5·4	0·68	0·10	0·83	0·0045	0·0045	2
4·1	1500	4·5	4·6	0·53	0·18	0·90	0·0039	0·0040	4
8·4	3100	4·7	4·4	0·54	0·33	0·85	0·0031	0·0033	8
12·6	4750	4·5	4·7	0·54	0·46	0·73	0·0027	0·003	12·8
16·7	6500	4·7	4·8	0·57	0·62	0·66	0·0028	0·0029	16
18·8	7100	4·8	4·8	0·55	0·69	0·65	0·0027	0·0028	19·2

TABLE 1. Summary of experimental conditions

hairpin eddies (Head & Bandyopadhyay 1978, 1979, 1981) and typical eddies† (Falco 1974, 1977).

2. Experimental information

A detailed description of the experimental arrangement, instrumentation and calibration procedures is given by Subramanian & Antonia (1981) and Subramanian (1981). The boundary layer developed with nominally zero pressure gradient over the smooth working section floor of the wind tunnel. The first 3 m of the floor were heated to provide a wall-heat-flux distribution that remained constant with x, the distance from the entrance to the working section. The boundary layer was tripped with a 3 mm diameter wire at $x = 40$ mm. The trip location was such that the virtual origins of the momentum and thermal layers were approximately coincident at all values of R_m used for the investigation.

Simultaneous measurements of u, v, θ were made, at several values of y/δ with an X-wire and a cold wire located 1·2 mm upstream of the X-wire centre and perpendicular to the X-wire plane. The X-wire/cold-wire arrangement was calibrated in the heated core of a plane jet. The hot wires (Pt–10 % Rh, 5 μm diameter) were operated at an overheat ratio of 1·8 with DISA 55M10 constant-temperature anemometers and linearized with DISA 55M25 units. The cold wire (Pt–10 % Rh, 0·6 μm diameter) was operated with a constant-current (0·1 mA) anemometer. Simultaneous records of temperature fluctuations at 11 positions across the layer were obtained with a rake of 11 cold wires (0·6 μm diameter) covering a relatively large range (nominally $0{\cdot}01 < y/\delta < 0{\cdot}9$) of the layer. Signals from the X-wire/cold wire and the rake were digitized at a sampling frequency f_s which varied (table 1) between 2 kHz ($R_m = 990$) and 19·2 kHz ($R_m = 7100$). The record duration was about 64 s at $R_m = 990$ and 13 s at $R_m = 7100$. To correct for the longitudinal separation between the X-wire and the cold wire, a time delay equal to two sampling intervals (1 sampling interval $\equiv f_s^{-1}$) was applied to the digital θ-records.

All measurements were made at a distance $x = 2{\cdot}24$ m for six values of U_1 or Reynolds number R_m. A summary of experimental conditions is given in table 1. Included in this table are values of δ_T, the thermal layer thickness, the momentum

† Head & Bandyopadhyay (1979) noted that the typical eddy features are precisely those one would expect to observe with a longitudinal light plane intersecting vortex loops or hairpin eddies close to the plane of symmetry.

thickness δ_2 ($R_m \equiv U_1\delta_2/\nu$), the friction velocity U_τ ($\equiv \tau_w^{\frac{1}{2}}$, τ_w is the kinematic wall shear stress) and the friction temperature T_τ ($\equiv Q_w/U_\tau$, Q_w is the thermometric wall heat flux). The experimental skin friction c_f ($\equiv 2\tau_w/U_1^2$) values, also shown in the table, are in good agreement with those of Coles (1962) for all values of R_m.

Mean and r.m.s. velocity and temperature profiles were measured for all values of R_m, and are presented in Subramanian & Antonia (1981). The constants in the mean-velocity and temperature log laws were found to be independent of R_m. In the outer layer the maximum departures from these log laws increased as R_m increased between 900 and 4000. For $R_m \gtrsim 4000$ these departures, which have been interpreted as measures for the strength of the 'wake' components, are approximately constant. Scaling of r.m.s. velocity and temperature distributions on inner-layer variables (U_τ and ν/U_τ are the characteristic velocity and length scale respectively) was reasonable and independent of R_m only for $y^+ \lesssim 15$. In the outer layer, scaling of these distributions on outer layer variables was satisfactory for $R_m \gtrsim 3000$.

3. Conditional technique

Subramanian *et al.* (1981) made a detailed comparison between several conditional techniques used to detect temperature fronts on the basis of information at one point in the flow and the identification of the fronts by visual inspection of the rake signals. Relatively poor agreement, in terms of correspondence of fronts,was found between the visual inspection approach (called RAKE by Subramanian *et al.*) and the one-point conditional techniques. This result was somewhat similar to that of Offen & Kline (1973), who found that none of the one-point detection schemes they investigated correlated well with the flow-visualization indication of 'bursts'. For the present investigation, which is more concerned with qualitative than quantitative effects of R_m on the boundary-layer structure, the VITA (variable-interval time-averaging) technique was used to obtain conditional averages of u, v, θ and their products. Of the conditional techniques considered by Subramanian *et al.* (1981), VITA and the conditional technique used by Rajagopalan & Antonia (1981) were found to correlate best with the visual identification of fronts from the rake signals. The implementation of the visual identification was cumbersome in view of the relatively large number of fronts (typically 400) required for satisfactory convergence of the conditional averages. It should be noted however that Subramanian *et al.* (1981) found that VITA and other one-point techniques led to averages in qualitative agreement with those obtained with the visual identification. Preliminary results obtained (Antonia *et al.* 1980) using RAKE for a relatively small number of fronts and three values of R_m are in good agreement with the VITA results presented in §4.

In VITA the identification of the front occurs whenever the two conditions $\dot{\tilde{\theta}} < 0$ and $\tilde{\theta}^2 - \tilde{\theta}^2 > k\theta'^2$ are satisfied. The prime denotes an r.m.s. quantity, the dot denotes differentiation with respect to time, and the tilde denotes averaging over a time interval τ, such that

$$\tilde{\theta} = \tau^{-1}\int_{t-\frac{1}{2}\tau}^{t+\frac{1}{2}\tau} \theta(t)\,dt.$$

The particular values of the parameters k and τ used here ($k = 0{\cdot}6$ and $\tau U_1/\delta \simeq 0{\cdot}09$) were selected when the X-wire/cold-wire arrangement was at one particular value of

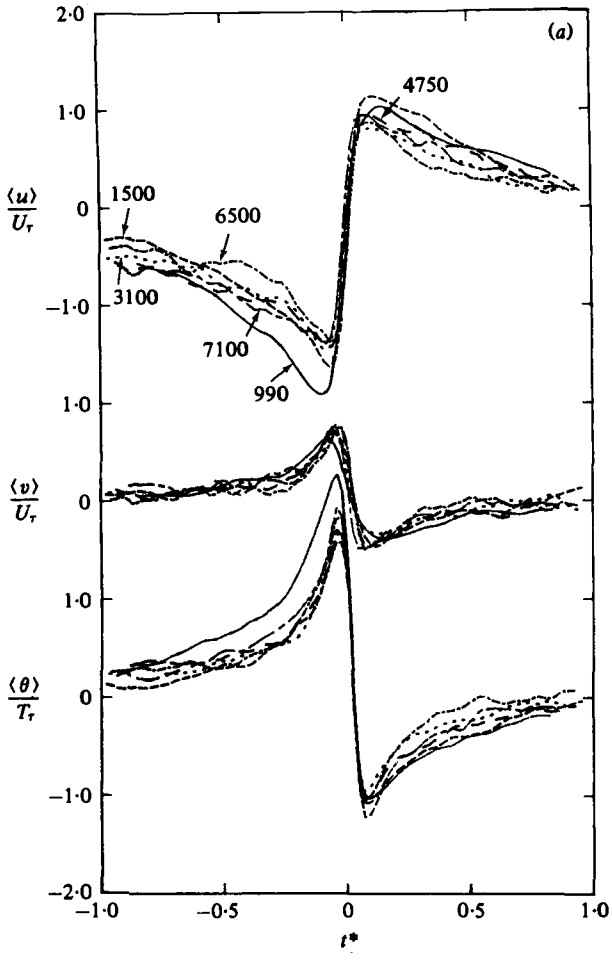

FIGURE 1(*a*). For caption see p. 130.

y/δ ($\simeq$ 0·3) and for R_m = 3100. The selection was made to provide agreement, at this particular Reynolds number, between the number of fronts obtained with VITA and that obtained with RAKE. These values of k and τ were unchanged for all values of y/δ and R_m. Conditional averages, presented in §4, are ensemble averages (the number of fronts in the ensemble is 400), denoted by angular brackets, with $t = 0$ arbitrarily identified with the time at which the fronts are aligned.

4. Conditional averages associated with front

Conditional averages of u, v, θ are shown in figure 1 for $y/\delta \simeq 0{\cdot}3$–$0{\cdot}9$, at all values of R_m. Velocity and temperature have been normalized by U_τ and T_τ respectively. These scales are considered here as adequate characteristic scales for the outer layer. Time t has been multiplied by U_1/δ ($t^* = tU_1/\delta$), a normalization also used by Chen & Blackwelder (1978). Some justification for this normalization is provided by measurements (Subramanian & Antonia 1979) of the convection velocity U_c of the front. These measurements, over the range $0{\cdot}1 < y/\delta < 1{\cdot}1$, showed no dependence on R_m. They

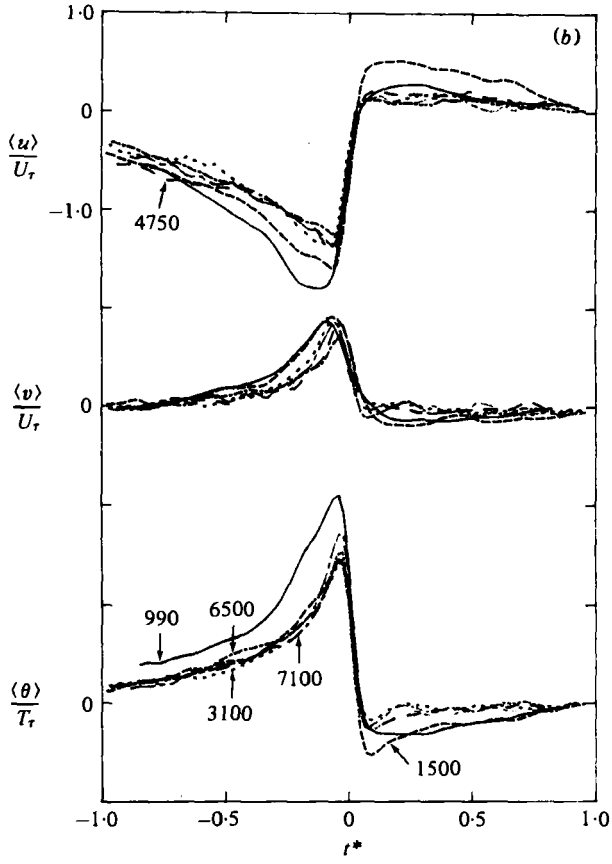

FIGURE 1(*b*). For caption see p. 130.

also indicated that the local mean velocity U was a reasonable approximation to U_c,† although, over the range $0{\cdot}7 \leqslant y/\delta \leqslant 1{\cdot}0$, the free-stream velocity U_1 was as close an approximation to U_c as U. U_1 has been used here to form a length scale tU_1, but the use of U instead of U_1 does not affect the results in this section.

Figure 1 indicates that the sudden decrease in temperature near $t^* = 0$ is accompanied by relatively large changes in $\langle u \rangle$ and $\langle v \rangle$. The conditional average $\langle v \rangle$ is in phase with $\langle \theta \rangle$, while $\langle u \rangle$ and $\langle \theta \rangle$ (or $\langle v \rangle$) are essentially out of phase. As y/δ increases $\langle v \rangle$ and $\langle \theta \rangle$ become more positively skewed while $\langle u \rangle$ becomes more negatively skewed. At $y/\delta = 0{\cdot}8$ and $0{\cdot}9$, $\langle \theta \rangle$ assumes, almost immediately following the sudden decrease at $t^* = 0$, a constant value corresponding to the ambient temperature of the free stream. The main feature of figure 1 is the reasonable collapse, for $t^* < 0$, of conditional averages for $R_m > 3100$.‡ The departure of signatures at $R_m = 990$ is marked at all values of y/δ, except perhaps for $\langle v \rangle$ and $y/\delta = 0{\cdot}3$. At $y/\delta = 0{\cdot}9$, averages at both $R_m = 990$ and 1500 differ perceptibly from those at higher Reynolds numbers. The averages at $R_m = 990$ and 1500 are larger in amplitude and cross the negative t^* axis at larger values of t^* than those at higher R_m.

† Phong-Anant *et al.* (1980) found that the local wind velocity was a good approximation to U_c in the atmospheric surface layer.

‡ The use of r.m.s. values of u, v and θ instead of U_τ and T_τ does not affect this collapse.

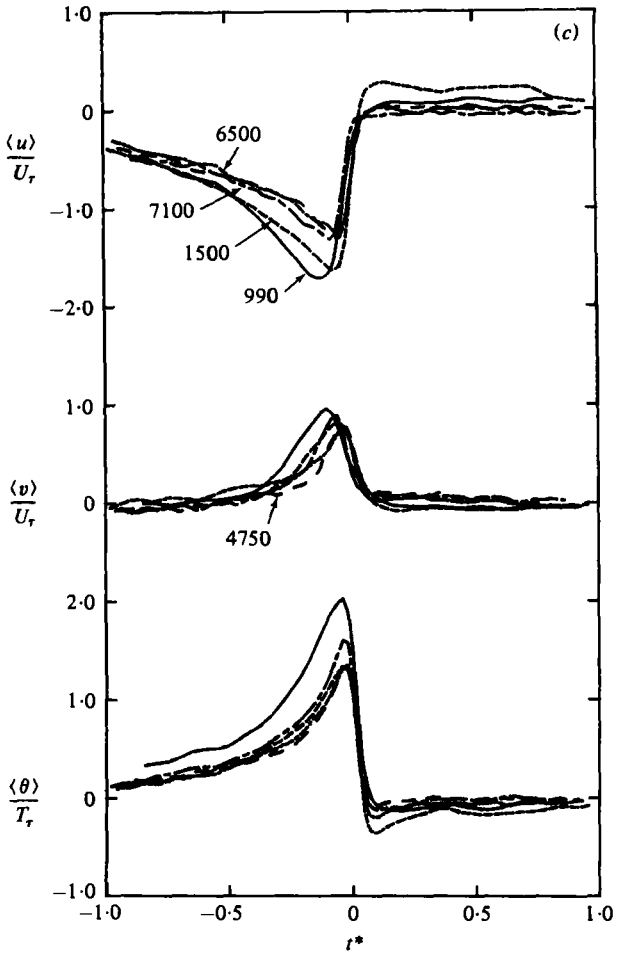

FIGURE 1(*c*). For caption see p. 130.

Conditional averages (figure 2) of products uv, $u\theta$, $v\theta$, at $y/\delta = 0{\cdot}9$ show that the difference between distributions at $R_m = 990$ or 1500 and higher R_m is quite marked and that the magnitude of averages at $R_m = 990$ is larger than at 1500. The collapse of averages at the higher R_m is not as good (this is particularly evident for $\langle u\theta \rangle$) as that observed for individual signatures (figure 1), apparently reflecting the greater sensitivity of products to the criteria used in the conditional technique. In figure 2 the maximum values of $\langle -uv \rangle$ and $\langle v\theta \rangle$ at $R_m = 990$ represent roughly 60 % of the wall shear stress and wall heat flux respectively. The maximum value of $\langle u\theta \rangle$ is twice the wall heat flux. It should be noted that conditional averages of products obtained within or immediately outside the inner layer indicate practically no R_m dependence.

The observed existence of the front across almost the entire boundary layer prompted Chen & Blackwelder (1978) to suggest that the front may provide the dynamical link between the outer-layer bulges and the bursting phenomenon near the wall. While most of the results in this section pertain to the outer layer, it seems pertinent to compare conditional averages obtained in the outer layer with those near the wall. The smallest value of y^+ that could be achieved with the present X-wire/

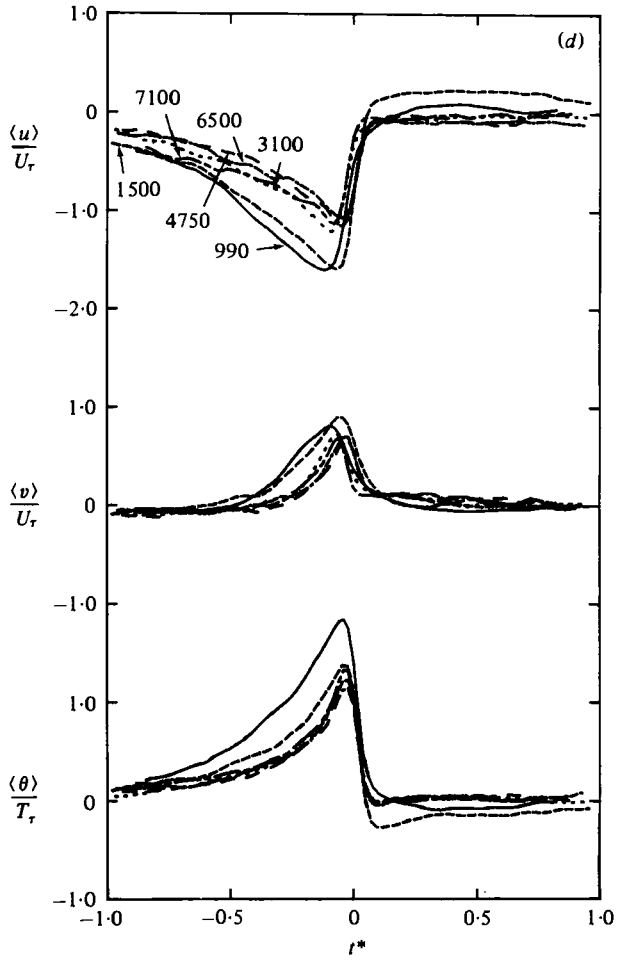

FIGURE 1. Conditional averages of u, v, θ in the outer layer. ——, R_m = 990; - - - - -, 1500; · · · · · ·, 3100; - - –, 4750; — · —, 6500; — → —, 7100. (*a*) y/δ = 0·3; (*b*) 0·7; (*c*) 0·8; (*d*) 0·9.

cold-wire arrangement was approximately 15 for $R_m = 990$. Conditional averages at $y^+ = 15, 37, 75$ are shown in figures 3 and 4. The most interesting feature is the relatively sudden change in the behaviour of the products as y^+ increases from 15 to 37: the large peak ($y^+ = 15$) at $t^* \simeq +0{\cdot}1$ decreases considerably, while a smaller increase is observed in the magnitude of the peak (at least in the case of $\langle uv \rangle$ and $\langle v\theta \rangle$) at $t^* \simeq -0{\cdot}2$. It is possible that the maxima of the conditional products, on either side of $t^* = 0$, reflect the importance of ejection ($\langle u \rangle$ is negative, $\langle v \rangle$ and $\langle \theta \rangle$ are positive) and sweep events ($\langle u \rangle$ is positive, $\langle v \rangle$ and $\langle \theta \rangle$ are negative) identified by previous investigators (e.g. Wallace, Eckelmann & Brodkey 1972; Willmarth & Lu 1972) with the second ($u < 0$, $v > 0$) and fourth quadrants respectively of the (u, v)-plane. The large values of $\langle uv \rangle$, $\langle v\theta \rangle$ and, in particular, $\langle -u\theta \rangle$ would suggest that the sweep becomes dominant as the wall is approached. This suggestion is consistent with both flow-visualization results and measured conventional and conditional statistics of velocity and temperature fluctuations near the wall. While the results of figure 4 are in qualitative agreement with the fully developed duct flow (with a thick viscous

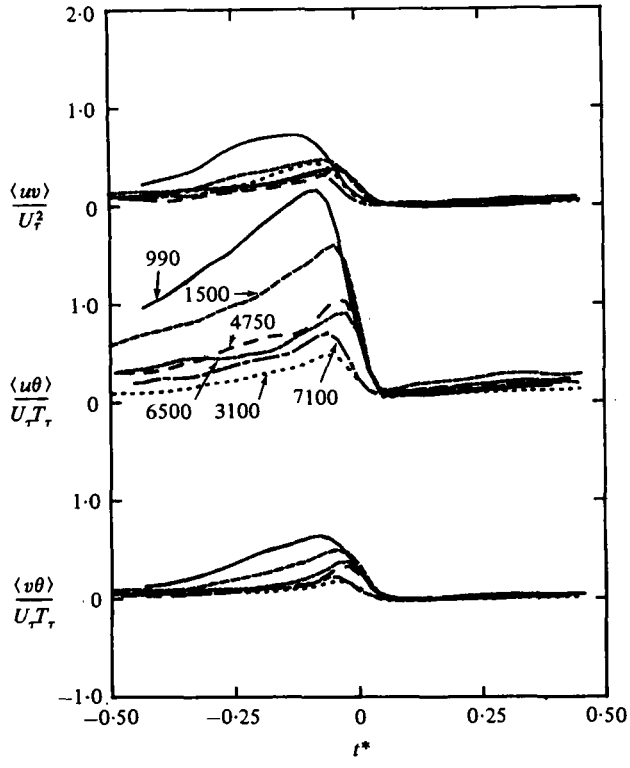

FIGURE 2. Conditional averages of products uv, $u\theta$ and $v\theta$ at $y/\delta = 0{\cdot}9$. Symbols are as in figure 1.

sublayer) measurements of Wallace, Brodkey & Eckelmann (1977), the latter results (R_m is estimated to be about 500) suggest that the sweep dominates at distances closer to the wall than implied by figure 4. The normalized and ensemble-averaged $\langle uv \rangle$ patterns of Wallace *et al.* (1972) indicated that the sweep was practically the only event occurring at $y^+ \simeq 3$. At $y^+ \simeq 10$, a double contribution was noticeable and, at $y^+ \simeq 15$, the contribution due to the ejection was larger than that due to the sweep. The results of figure 3 tend to underline the importance of the ejection event in the outer part of the layer, especially at the smaller R_m. It should perhaps be noted here that the term 'ejection' is used in the same sense as by Lu & Willmarth (1973), and does not necessarily imply a direct connection with the physically observed ejection, away from the wall, of low-momentum fluid.

An interesting feature of figure 3 is the approximate coincidence of zero crossings for $\langle u \rangle$, $\langle v \rangle$, $\langle \theta \rangle$ at y^+ of 37 and 75. This approximate coincidence is observed at larger values of y/δ and supports the association, suggested by Chen & Blackwelder (1978), between the temperature front and the internal 'shear layer'. These authors noted, however, that as the wall is approached ($y/\delta \lesssim 0{\cdot}1$) the zero crossings of $\langle u \rangle$ and $\langle v \rangle$ occurred earlier than the zero crossing of $\langle \theta \rangle$. This phase shift could not be explained, but it was speculated that the shift could perhaps be attributed to an aspect of the eddy structure, such as the streamwise vortices, that was not measurable with their probes. While the present results at $y^+ = 15$ indicate that $\langle u \rangle$ and $\langle v \rangle$ cross zero in advance of $\langle \theta \rangle$, the shift corresponds to approximately 0·04 (on the t^* scale), which is smaller than the VITA filtering time of 0·09 ($\equiv \tau^*$). As one sampling time interval

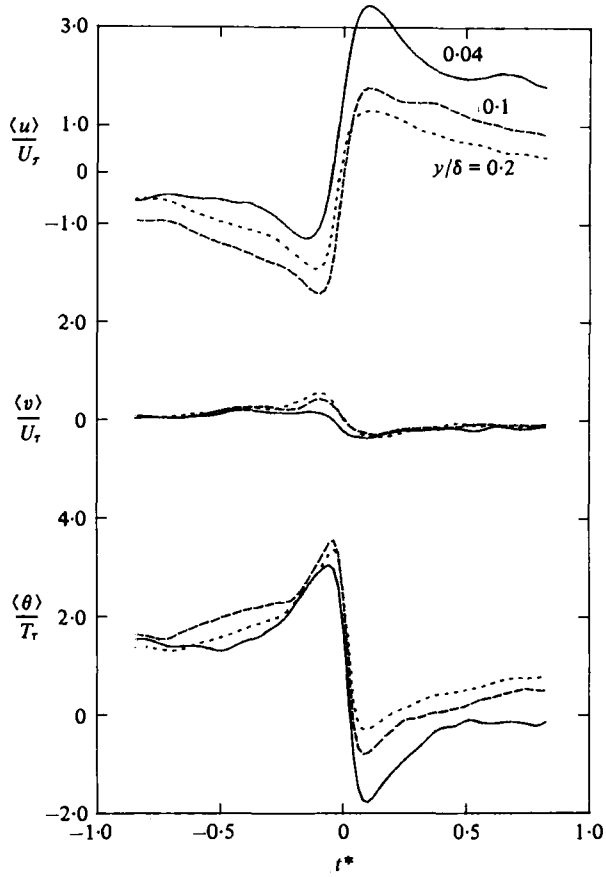

FIGURE 3. Conditional averages of u, v, θ in the inner layer at $R_m = 990$. ——, $y/\delta = 0{\cdot}04$, $y^+ = 15$; — —, 0·1, 37; - - -, 0·2, 75.

corresponds to approximately 0·02 on the t^* scale at $R_m = 990$, the difference in zero crossings cannot be considered as significant. Nevertheless, the possibility of a shift for $y^+ < 15$ cannot be ruled out entirely.

5. Other characteristics of front

The mean period $\bar{T}$ ($\bar{T}^* \equiv \bar{T}U_1/\delta$) between fronts is plotted in figure 5 as a function of R_m for several values of y/δ. In the outer layer, $\bar{T}^*$ is approximately constant for $R_m \geqslant 1500$. At $y/\delta = 0{\cdot}04$, $\bar{T}^*$ increases rapidly when R_m decreases below 3000, and is about 44 at $R_m = 990$. This Reynolds-number behaviour is consistent (Antonia *et al.* 1980) with the results obtained by counting the fronts that are visually detected (RAKE) in the rake-temperature signals. The slight increase in $\bar{T}^*$ with y/δ is a consequence of fixing the values of k and τ in VITA. At any particular R_m, one value only of $\bar{T}^*$ is inferred from RAKE since, by definition, the front is counted only when it is detected over a relatively large range of y/δ. The RAKE value of $\bar{T}^* \simeq 2{\cdot}5$ is in reasonable agreement with the value of about 2·6 inferred from the front-crossing frequency, also obtained with VITA, by Chen & Blackwelder (1978) at $R_m = 2800$. Lu & Willmarth

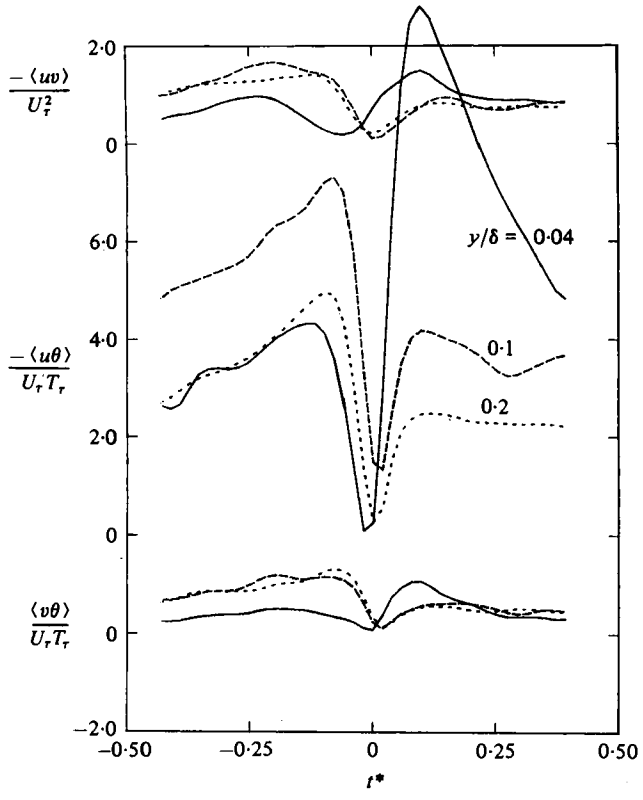

FIGURE 4. Conditional averages of products uv, $u\theta$, $v\theta$ in the inner layer at $R_m = 990$. Symbols are as in figure 3.

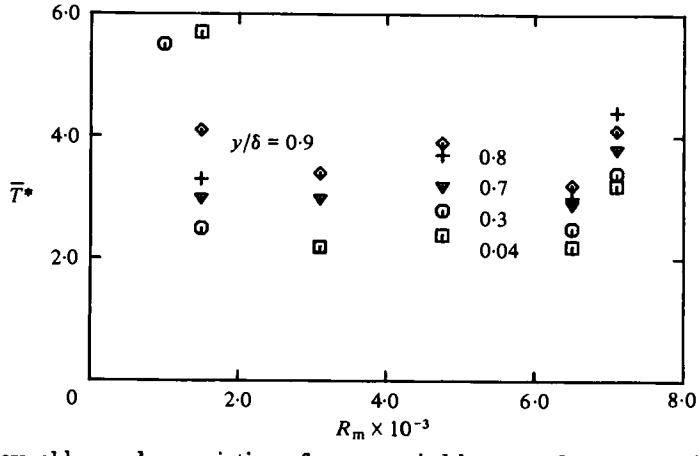

FIGURE 5. Reynolds-number variation of mean period between fronts. ⊡, $y/\delta = 0{\cdot}04$; ⊙, 0·3; ▼, 0·7. At $R_m = 990$, $\bar{T}^* = 7{\cdot}6$ at $y/\delta = 0{\cdot}7$ and 43·6 at $y/\delta = 0{\cdot}04$.

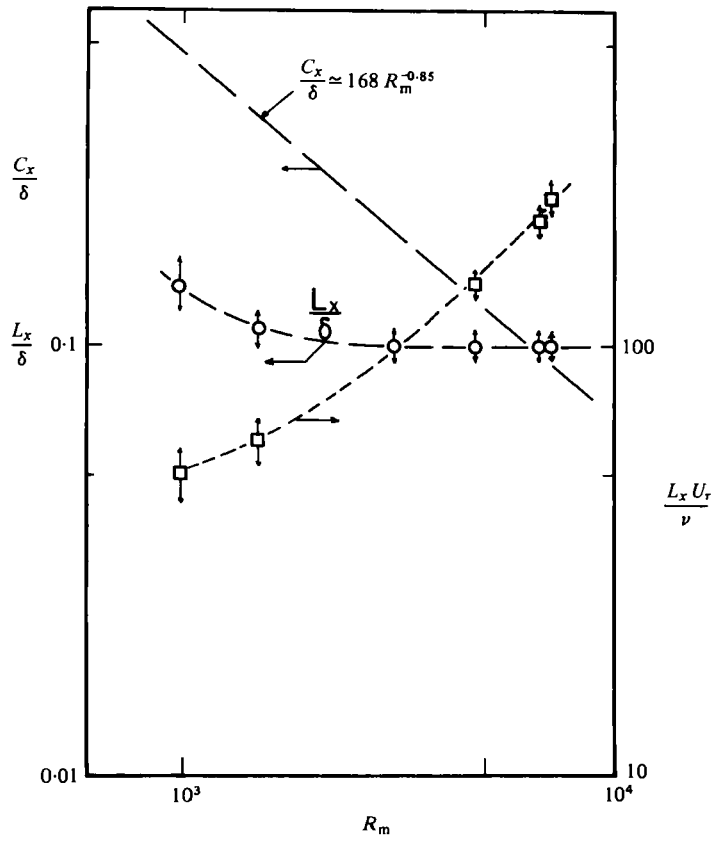

FIGURE 6. Streamwise length scale of temperature front. ○, L_x/δ; □, $L_x U_\tau/\nu$; - - -, C_x/δ, streamwise length scales of typical eddies (Falco 1974). Extent of arrows indicates the maximum variation over the range $0{\cdot}1 \leqslant y/\delta \leqslant 0{\cdot}8$.

(1973), by dividing the (u, v)-plane into five regions (the central region was called the hole, with a size determined by the curves $|uv| =$ constant), found that the mean period $\overline{T}_e$ of ejections was given by $\overline{T}_e^* = 5$ when the hole size H ($\equiv |uv|/u'v'$) was set equal to 4·5. A value of H of about 1·9 would yield a value of $\overline{T}_e^* \simeq 2{\cdot}5$. Verification for this value of H was provided by Subramanian *et al.* (1981), who found approximate agreement between the hole-crossing frequency and the frequency of visually recognized fronts in the rake signals.

A measure of the streamwise length scale of the front can be obtained from the difference Δt between locations of the negative and positive peaks, on either side of $t = 0$, of conditionally averaged temperatures or velocities. If the product $U_1 \Delta t$ is identified with the streamwise length L_x of the front, the ratio L_x/δ (figure 6), determined from the $\langle\theta\rangle$ distributions, is approximately independent of R_m (the independence of L_x/δ on y/δ has been established for values of y/δ extending to 0·9), and equal to about 0·1, when R_m is greater than about 3000. Chen & Blackwelder (1978) also obtained $L_x/\delta = 0{\cdot}1$ at $R_m = 2800$. It is of interest to note that, as a proportion of the Kolmogorov microscale η, L_x increases from about 15η at $R_m = 990$ to 37η at $R_m = 7100$.

Falco (1974) found that, for $900 < R_m < 20000$, the length scale C_x of the typical

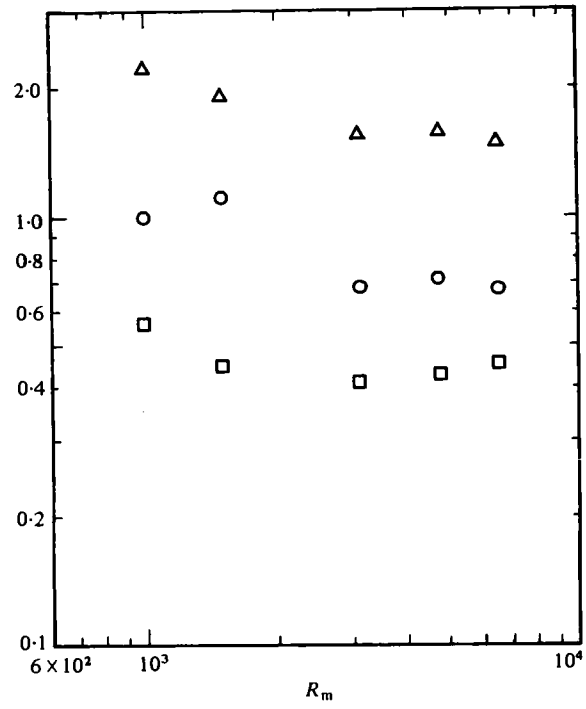

FIGURE 7. Velocity and temperature gradients across the fronts. ○, $U_1^{-1}(\partial\langle u\rangle/\partial t^*)_{max}$; □, $U_1^{-1}(\partial\langle v\rangle/\partial t^*)_{max}$; △, $(T_w - T_1)^{-1}\,(\partial\langle\theta\rangle/\partial t^*)_{max}$.

eddy decreased continuously, as a proportion of δ, with increasing R_m according to $C_x/\delta \simeq 168R_m^{-0.85}$ (shown in figure 6). Falco's suggestion that C_x scaled with the Taylor microscale λ cannot be reconciled with the experimental variation of λ/δ with R_m or R_δ ($\equiv U_1\delta/\nu$). With the assumption that production and dissipation of turbulent energy are approximately in balance (the energy budgets measured by Murlis (1975), who obtained the dissipation by difference, support this assumption over a range of R_m), it is easy to show that, in the outer layer, λ/δ should vary as $R_m^{-0.5}$ and not as $R_m^{-0.85}$. Falco's (1977) result that $C_x U_\tau/\nu$ is constant cannot, in any case, be reconciled with the result (Falco 1974) that C_x/λ is constant, since $\lambda U_\tau/\nu$ varies as $(U_\tau/U_1)\,R_\delta^{\frac{1}{2}}$, and is therefore Reynolds-number-dependent. The result that $C_x U_\tau/\nu$ is constant contrasts with the relatively rapid increase with Reynolds number (figure 6) of the ratio $L_x U_\tau/\nu$.

Murlis *et al.* (1980) found that the most probable turbulent bulge length B_x, derived from temperature intermittency statistics, is approximately independent of y, but decreases strongly as R_m increases. The ratio $B_x U_\tau/\nu$ remained approximately constant ($\simeq$ 120), independent of R_m (the data extended to $R_m \simeq 5000$). It was suggested that this constancy supported the constancy of $C_x U_\tau/\nu$, the typical eddies being identified with the small-scale undulations of the viscous superlayer. The measurements of Murlis *et al.* and those of Andreopoulos (1978) at $R_m \simeq 22000$ suggest that the average length and average frequency of turbulent bulges is consistent, when δ and U_1 are used as normalizing scales, with the established Reynolds-number independence of most outer-layer statistics for $R_m \gtrsim 5000$ (note that the variation in the range $3000 \lesssim R_m \lesssim 5000$ is only small). The implied constancy of $C_x U_\tau/\nu$ (and the implication that

$B_x U_\tau/\nu$ is constant for $R_m > 5000$) would be reconcilable with the Reynolds-number independence of conventional averages only if the viscosity-dependent typical eddies make a negligible contribution to the Reynolds stresses for $R_m > 5000$. This last condition would need to be reconciled with Falco's (1974) claim that entrainment at large R_m continues to take place on typical eddy scales.

Maximum values of temperature and velocity gradients associated with the front were obtained (figure 7) at $y/\delta = 0{\cdot}7$ and all values of R_m. These maximum values are approximately constant over a small region centred at or near $t^* = 0$. Since quantitative agreement between ensemble averages obtained using different conditional techniques is poor (Subramanian *et al.* 1981), the precise magnitude of these maximum values is not important here. It has also been established that, even when one particular technique is used, the magnitude of the averages may depend on the particular signal used in the detection criterion. For example when VITA is used an enhancement of the magnitude of $\langle u \rangle$ would result if θ were replaced by u in the detection criterion. Such enhancement might change the magnitude of all derivatives in figure 7, but should not affect the Reynolds-number variation indicated in the figure. The magnitudes of the derivatives in figure 7 become approximately constant for $R_m \gtrsim 3000$, a result which is consistent with the indicated constancy in figure 6 of L_x/δ when $R_m \gtrsim 3000$. It is interesting to note that the magnitude of the derivatives of $\langle u \rangle$ and $\langle v \rangle$ across the front is of order U_1/δ. Head & Bandyopadhyay (1979, 1981) suggested that the inclination of the hairpin vortices might coincide with the direction of the principal rate-of-strain axes of the flow. This suggestion would seem to be consistent with the suggestion by Townsend (1956) that the eddies that are effective in extracting energy from the mean flow are those that are approximately aligned with the principal axis of the mean rate of strain. The magnitude of the principal rate of strain is $\frac{1}{2}(\partial U/\partial y)$ and is of order U_1/δ across the boundary layer. For $R_m \simeq 7000$, we estimate that the principal rate of strain decreases continuously from about unity at $y/\delta \simeq 0{\cdot}05$ to zero at the edge of the layer. It seems therefore that the velocity derivative across the front, which is approximately constant across the layer, assumes the magnitude of the maximum rate of strain in the near-wall region of the layer.

6. Comparison with typical eddies

Falco (1977) inferred that the Reynolds-number-dependent typical eddies produced most of the Reynolds stress in the outer half of the layer at $R_m \simeq 1200$ and that they are formed on the upstream side of the large-scale motions at all Reynolds numbers investigated. Chen & Blackwelder (1978) noted that, in the outer intermittent region, the temperature front was always associated with the upstream side or back of the turbulent bulges. It is not clear whether these bulges are immediately identifiable with the large-scale motions which Falco associated with 'the existence of smoke-free regions or concentration gradients which extend deep into the layer on both the upstream and downstream side of the bulges'. These motions have an average length of $1{\cdot}6\delta$, while the average bulge length, as inferred for example by Kovasznay, Kibens & Blackwelder (1970) and Antonia (1972) from measured intermittency factor and intermittency frequency distributions, decreases from about $1{\cdot}7\delta$ at $y/\delta \simeq 0{\cdot}6$ to $0{\cdot}2\delta$ at $y/\delta \simeq 1{\cdot}0$. In his model of the outer region, Falco (1977) shows large-scale motions with an average streamwise spacing of about $2{\cdot}5\delta$. The agreement between

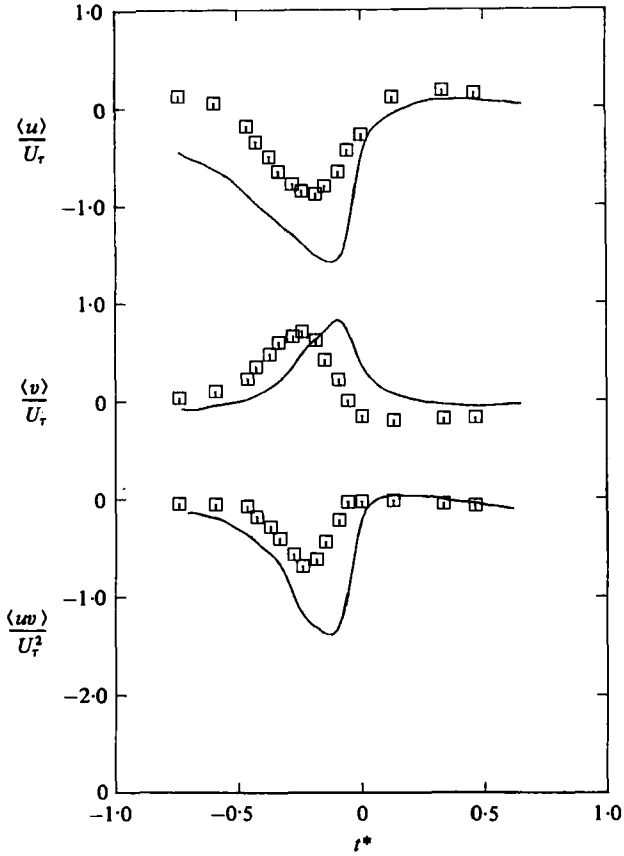

FIGURE 8. Comparison of conditional averages of u, v, uv with typical eddy averages. ——, $R_m = 990$, $y/\delta = 0{\cdot}9$; □, Falco (1977), $R_m = 1200$, $y/\delta = 0{\cdot}87$.

this spacing and that of the fronts would suggest that the association of the fronts with the upstream interfaces of the large-scale motions is not unreasonable. It therefore seems reasonable to compare conditional averages associated with fronts with those associated with typical eddies. Falco conditionally sampled signals from an X-wire with respect to the passage of a typical eddy and presented ensemble-averaged distributions at $y/\delta = 0{\cdot}87$ ($R_m \simeq 1200$) of $\langle u\rangle$, $\langle v\rangle$ and $\langle uv\rangle$ as functions of time normalized by the average duration of a typical eddy. These averages were compared with ensemble averages obtained by Antonia (1972) at $y/\delta = 0{\cdot}95$. Since all turbulent bulges were included for these latter ensemble averages, it is not surprising that the peak values of $\langle u\rangle/U_\tau$, $\langle v\rangle/U_\tau$ and $-\langle uv\rangle/U_\tau^2$ obtained by Falco were larger (by about 75% in the case of $-\langle uv\rangle/U_\tau^2$) than those of Antonia (1972). It would seem more meaningful to compare Falco's typical eddy signatures with those associated with the temperature front. Such a comparison is presented in figure 8. The present distributions were obtained at $y/\delta \simeq 0{\cdot}9$ for $R_m = 990$. To display Falco's averages in figure 8, it was assumed that $t^* = 0$ coincides with the back of a typical eddy and that the relevant length scale of this eddy was equal to $0{\cdot}41\delta$,† a result obtained using $C_x/\delta \simeq 168 R_m^{-0{\cdot}847}$ for $R_m = 1200$.

† Using $C_x U_\tau/\nu \simeq 200$, C_x/δ was estimated to be about 0·38 at $R_m \simeq 1200$.

The VITA signatures (figure 8) are comparable in extent to the typical eddy signatures. The maximum value of $-\langle uv\rangle/U_\tau^2$ for VITA is about twice that for the typical eddy. Falco inferred, from the typical eddy $\langle uv\rangle$ signature, that the typical eddy contributed most of the Reynolds shear stress at $R_\mathrm{m} \simeq 1200$. The magnitude of this contribution was not estimated, presumably since the typical eddy frequency does not appear to have been estimated. A crude estimate of the contribution to the Reynolds shear stress of the structure characterized by the front can be obtained by integrating the present $\langle uv\rangle$ signature over a period corresponding to the mean interval $\overline{T}$ between fronts. Since $\langle uv\rangle$ is approximately zero at $t^* = 0$ and at $t^* = -1$, the contribution to $\overline{uv}$ is assumed to be given by

$$\frac{U_\tau^2}{\overline{T}^*\overline{uv}}\int_{-1}^{0}\frac{\langle uv\rangle}{U_\tau^2}\,dt^*,$$

and is about 0·5. If the present values of $\overline{T}^*$ ($\simeq 6$) and $-\overline{uv}/U_\tau^2$ ($\simeq 0{\cdot}14$) are assumed to apply to Falco's conditions, the contribution of the typical eddy to $-\overline{uv}$ is estimated to be about 0·2. The contribution of the typical eddy to $-\overline{uv}$ at larger Reynolds numbers is not easy to estimate. According to Falco (1974), C_x/δ is about 0·1 at $R_\mathrm{m} \simeq 6000$ and 0·06 at $R_\mathrm{m} \simeq 10000$. An optimistic estimate of the contribution to $-\overline{uv}$ can be obtained by integrating $\langle uv\rangle$ over the time interval corresponding to the passage time of the front (recall that $L_x/\delta \simeq 0{\cdot}1$ for $R_\mathrm{m} > 3000$). The resulting contribution is less than 0·05 at $R_\mathrm{m} = 7100$ (at $R_\mathrm{m} = 990$, the contribution is about 0·1), implying a negligible contribution of the viscosity-dependent typical eddy to the Reynolds shear stress at large Reynolds numbers.

7. Concluding remarks

The conditional averages presented in §4 and the characteristic length scale and velocity and temperature derivatives (§5) associated with the fronts seem to be fully consistent with the Reynolds-number independence, previously established in the literature, of conventional averages when R_m exceeds about 3000. At lower Reynolds numbers, the larger length scales are emphasized, as can be inferred from the increase (figure 6) of the length scale of the front and the increase in the duration of the velocity and temperature signatures in figure 1. For $R_\mathrm{m} < 3000$, L_x does not scale on δ.

The contribution to the Reynolds shear stress, at $R_\mathrm{m} = 990$, of the structure associated with the front is significant. It also seems likely that the contribution from the typical eddy at a Reynolds number comparable to the Reynolds shear stress cannot be ignored. The association between the structure characterized by the front and the typical eddy seems plausible at small Reynolds numbers.

Head & Bandyopadhyay (1981) have already remarked that the results of Chen & Blackwelder (1978) are in every way compatible with the smoke-flow visualization results. They also suggested that the interpretation of Chen & Blackwelder's results in terms of fronts was not necessarily warranted since the detailed similarities between the simultaneous temperature (or velocity) traces at different levels in the boundary layer are due to long narrow features extending through the boundary layer. The suggestion is not substantiated by the present results or those of Chen & Blackwelder, which tend to support the possibility that the front relates the outer large-scale motion

to the organized motion near the wall. At small Reynolds numbers, hairpin eddies have been identified with the large eddies, and the association between the structure characterized by the front and the hairpin eddy seems plausible. At higher Reynolds numbers, signatures associated with the front have a streamwise extent which scales on δ whereas cross-stream dimensions of hairpin eddies scale approximately with ν/U_τ, in agreement with typical eddy scaling. A direct association between the structure characterized by the front and the hairpin and typical eddies seems tenuous when R_m is greater than about 1500.

The support of the Australian Research Grants Committee is gratefully acknowledged. The authors are grateful to Dr D. H. Wood for his valuable comments.

REFERENCES

ANDREOPOULOS, J. 1978 Symmetric and asymmetric near wake of a flat plate. Ph.D. thesis, Imperial College, University of London.

ANTONIA, R. A. 1972 Conditionally sampled measurements near the outer edge of a turbulent boundary layer. *J. Fluid Mech.* **56**, 1–18.

ANTONIA, R. A., SUBRAMANIAN, C. S., RAJAGOPALAN, S. & CHAMBERS, A. J. 1980 Reynolds number dependence of the large structure in a slightly heated turbulent boundary layer. Presented at *ICHMT/IUTAM Symp. on Heat & Mass Transfer and the Structure of Turbulence, Dubrovnik.*

BANDYOPADHYAY, P. 1980 Large structure with a characteristic upstream interface in turbulent boundary layers. *Phys. Fluids* **23**, 2326–2327.

BLACKWELDER, R. F. 1978 The bursting process in turbulent boundary layers. In *Coherent Structure of Turbulent Boundary Layers; AFOSR/Lehigh University Workshop* (ed. C. R. Smith & D. E. Abbott); pp. 211–224.

CHEN, C. H. P. 1975 The large scale motion in a turbulent boundary layer: a study using temperature contamination. Ph.D. thesis, University of Southern California.

CHEN, C.-H. P. & BLACKWELDER, R. F. 1978 Large-scale motion in a turbulent boundary layer: a study using temperature contamination. *J. Fluid Mech.* **89**, 1–31.

COLES, D. 1962 The turbulent boundary layer in a compressible fluid. *Rand Corporation Rep.* R-403-PR, ARC 24478.

FALCO, R. E. 1974 Some comments on turbulent boundary layer structure inferred from the movements of a passive contaminant. *A.I.A.A. Paper* no. 74-99.

FALCO, R. E. 1977 Coherent motions in the outer region of turbulent boundary layers. *Phys. Fluids Suppl.* **20**, S124–S132.

FALCO, R. E. 1979 Comments on "Large structure in a turbulent boundary layer". *Phys. Fluids* **22**, 2042–2043.

HEAD, M. R. & BANDYOPADHYAY, P. 1978 Combined flow visualisation and hot-wire measurements in turbulent boundary layers. In *Coherent Structure of Turbulent Boundary Layers; AFOSR/Lehigh University Workshop* (ed. C. R. Smith & D. E. Abbott); pp. 98–125.

HEAD, M. R. & BANDYOPADHYAY, P. 1979 Flow visualisation of turbulent boundary layer structure. *AGARD Conf. Proc.* CP271, 25.1–25.12.

HEAD, M. R. & BANDYOPADHYAY, P. 1981 New aspects of turbulent boundary-layer structure. *J. Fluid Mech.* **107**, 297–338.

HUFFMAN, G. D. & BRADSHAW, P. 1972 A note on von Kármán's constant in low Reynolds number turbulent flows. *J. Fluid Mech.* **53**, 45–60.

KOVASZNAY, L. S. G., KIBENS, V. & BLACKWELDER, R. F. 1970 Large scale motion in the intermittent region of a turbulent boundary layer. *J. Fluid Mech.* **41**, 283–325.

LU, S. S. & WILLMARTH, W. W. 1973 Measurements of the structure of the Reynolds stress in a turbulent boundary layer. *J. Fluid Mech.* **60**, 481–512.

MURLIS, J. 1975 The structure of a turbulent boundary layer at low Reynolds number. Ph.D. thesis, Imperial College, University of London.

MURLIS, J., TSAI, H. M. & BRADSHAW, P. 1980 The structure of turbulent boundary layers at low Reynolds numbers. Private communication.

OFFEN, G. R. & KLINE, S. J. 1973 Experiments on the velocity characteristics of 'bursts' and on the interaction between the inner and outer regions of a turbulent boundary layer. *Rep.* MD-31, *Dept Mech. Engng, Stanford University.*

PHONG-ANANT, D., ANTONIA, R. A., CHAMBERS, A. J. & RAJAGOPALAN, S. 1980 Features of the organised motion in the atmospheric surface layer. *J. Geophys. Res.* **85**, 424–432.

PURTELL, L. P. 1978 The turbulent boundary layer at low Reynolds number. Ph.D. thesis, University of Maryland.

PURTELL, L. P., KLEBANOFF, P. S. & BUCKLEY, F. T. 1981 Turbulent boundary layer at low Reynolds number. *Phys. Fluids* **24**, 802–811.

RAJAGOPALAN, S. & ANTONIA, R. A. 1981 Properties of the large structure in a slightly heated turbulent mixing layer of a plane jet. *J. Fluid Mech.* **105**, 261–281.

SUBRAMANIAN, C. S. 1981 Some properties of the large scale structure in a slightly heated turbulent boundary layer. Ph.D. thesis, University of Newcastle, Australia.

SUBRAMANIAN, C. S. & ANTONIA, R. A. 1979 Some properties of the large structure in a slightly heated turbulent boundary layer. In *Proc. 2nd Int. Symp. on Turbulent Shear Flows, London*, pp. 4.18–4.21.

SUBRAMANIAN, C. S. & ANTONIA, R. A. 1981 Effect of Reynolds number on a slightly heated turbulent boundary layer. *Int. J. Heat Mass Transfer* **24**, 1833–1846.

SUBRAMANIAN, C. S., RAJAGOPALAN, S., ANTONIA, R. A. & CHAMBERS, A. J. 1981 Comparison of conditional sampling and averaging techniques in a turbulent boundary layer. *Rep.* TN FM58, *Dept of Mech. Engng, University of Newcastle.*

TOWNSEND, A. A. 1956 *The Structure of Turbulent Shear Flow.* Cambridge University Press.

WALLACE, J. M., BRODKEY, R. S. & ECKELMANN, H. 1977 Pattern-recognized structures in bounded turbulent shear flows. *J. Fluid Mech.* **83**, 673–693.

WALLACE, J. M., ECKELMANN, H. & BRODKEY, R. S. 1972 The wall region in turbulent shear flow. *J. Fluid Mech.* **54**, 39–48.

WILLMARTH, W. W. & LU, S. S. 1972 Structure of the Reynolds stress near the wall. *J. Fluid Mech.* **55**, 65–92.